International Journal of Nanoelectronics and Materials
Volume 16 (Special Issue) December 2023 [111-119]

A Study on Electrical Performance of SiC-based Self-switching Diode (SSD) as a High Voltage High Power Device

N. Z. A. A. Sha'ari[1], N. F. Zakaria[1,3,*], S. R. Kasjoo[1,4], M. N. Norizan[1,3], I. S. Mohamad[1,3], M. F. Ahmad[1], S. A. A. Rais[1], B. Poobalan[1,4], N. Sabani[1,4] and A. F. A. Rahim[5]

[1]Faculty of Electronic Engineering Technology, Universiti Malaysia Perlis (UniMAP), Perlis, Malaysia
[2]Advanced Communication Engineering (ACE), Centre of Excellence, UniMAP, Perlis, Malaysia
[3]Geopolymer and Green Technology (CEGeoGTech), Centre of Excellence, UniMAP, Perlis, Malaysia
[4]Centre of Excellence for Micro System Technology (MiCTEC), Universiti Malaysia Perlis, Perlis, Malaysia
[5]Faculty of Electrical Engineering, Universiti Teknologi MARA, Permatang Pauh, Pulau Pinang, Malaysia

ABSTRACT

The Self-switching Diodes (SSDs) have been primarily researched and used in low-power device applications for RF detection and harvesting applications. In this paper, we explore the potential of SSDs in high-voltage applications with the usage of Silicon Carbide (SiC) as substrate materials which offers improved efficiency and reduced energy consumption. Optimization in terms of the variation in the interface charges, metal work function, and doping concentration values has been performed by means of a 2D TCAD device simulator. The results showed that the SSD can block up to 600 V of voltage with an optimum interface charge value of 1013 cm^{-2}, making them suitable for higher voltage applications. Furthermore, it also found that the work function of the metal contact affected the forward voltage value, impacting the current flow in the device. Variation in doping concentrations also resulted in higher breakdown voltages and significantly increased forward current, leading to an increased power rating of 27 kW. In conclusion, the usage of 4H-SiC-based SSDs shows a usable potential for high-voltage applications with optimized parameters. The results from this research can facilitate the implementation of SSD in the development of high-power semiconductor devices for various industrial applications.

Keywords: Self-switching diode, optimization, device simulation, silicon carbide, Silvaco

1. INTRODUCTION

Self-switching diodes (SSDs) have garnered significant research attention globally due to their potential as zero-bias RF rectifiers [1–5]. These devices exploit their nonlinear current-voltage (IV) characteristics to rectify input signals. The rectification process relies on controlling the electric-field-independent region (depletion region) within the asymmetric channel of the SSD. In contrast to more complex alternatives like Schottky diodes, SSDs employ a simpler design featuring an L-shaped channel, achievable through techniques such as electron beam lithography and chemical etching. Notably, SSDs eliminate the need for additional components like junctions, doping, or a third gate terminal during fabrication [3]. Researchers have primarily explored the application of SSDs across the electromagnetic spectrum for communication and energy harvesting purposes [6]. This is achieved by utilizing on the device's low turn-on voltage advantage and leveraging high-mobility materials like graphene, InAs, and InGaAs [4].

* Corresponding authors: norfarhani@unimap.edu.my, mohdnatashah@unimap.edu.my

While SSDs are primarily recognized for their effectiveness as zero-bias diodes in low-power contexts, this report delves into their potential under higher-power conditions. The investigation aims to evaluate the viability of employing SSDs as diode rectifiers within high-power setups, with an emphasis on integrating Silicon Carbide (SiC) as the substrate material. SiC has favourable electrical and thermal properties which make it suitable for accommodating increased power levels, potentially enhancing power efficiency [7]. With a wide bandgap exceeding 3 eV, SiC-based power devices demonstrate the ability to endure high voltages [8] and switching frequencies, attributed to their high electron saturation velocity of up to 2×10^7 cm/s [9, 10]. This renders them suitable for applications requiring high power and high-temperature resilience.

In view of the absence of conclusive proof for the SSD's viability as high-voltage power devices, an extensive investigation was conducted on a SiC-based SSD by means of a Silvaco TCAD device simulator to have an insight into the electrical characteristic performance of the device in a high-power condition setup. Investigation of the proper physical and materials model of the structure, variation on the interface charge values, work functions of the metal contacts, and the doping concentration of 4H-SiC-based SSDs have been performed to further study the behaviour of the device. Through comprehending the behaviour of SiC-based SSDs, this study aims to enhance the understanding of the potential of these SiC-based SSDs as high-power devices, with a specific focus on achieving an application with the potential of handling a minimal breakdown voltage of 600 V.

2. MATERIAL AND METHODS

The simulation of SiC-based SSD has been performed by means of a 2D TCAD simulator with AlGaS and Si as the base materials. A SiO_2 dielectric layer was introduced underneath the SiC layer to mitigate quantum mechanical tunneling at the field plate boundary [10] which can lead to unintended and unpredictable current leakage between the gate electrode and the underlying semiconductor material in high-power device [11].

Figure 1 shows the top view of the SiC-based SSD with L-shaped SiO_2 trenches which create a conducting channel via the 4H-SiC layer. 4H-SiC has been chosen due to its compatibility to form Schottky contacts on two distinct surfaces: the Si-face (enriched with silicon) and the C-face (enriched with carbon). The Si-face is particularly well-suited for establishing Schottky contacts compared to the C-face [10]. Consequently, the implementation of a uniformly doped, low-concentration epitaxial layer (with n-type polarity) on 4H-SiC necessitates the implementation for ensuring the appropriate foundation for creating these SSDs. The channel width, channel length, and trench width are 20, 17, and 5 μm, respectively. These values are created bigger compared to optimized parameters values intended for low-power applications [12] to allow handling of higher current and enhance the device's ability to withstand higher voltages without breaking down [13, 14].

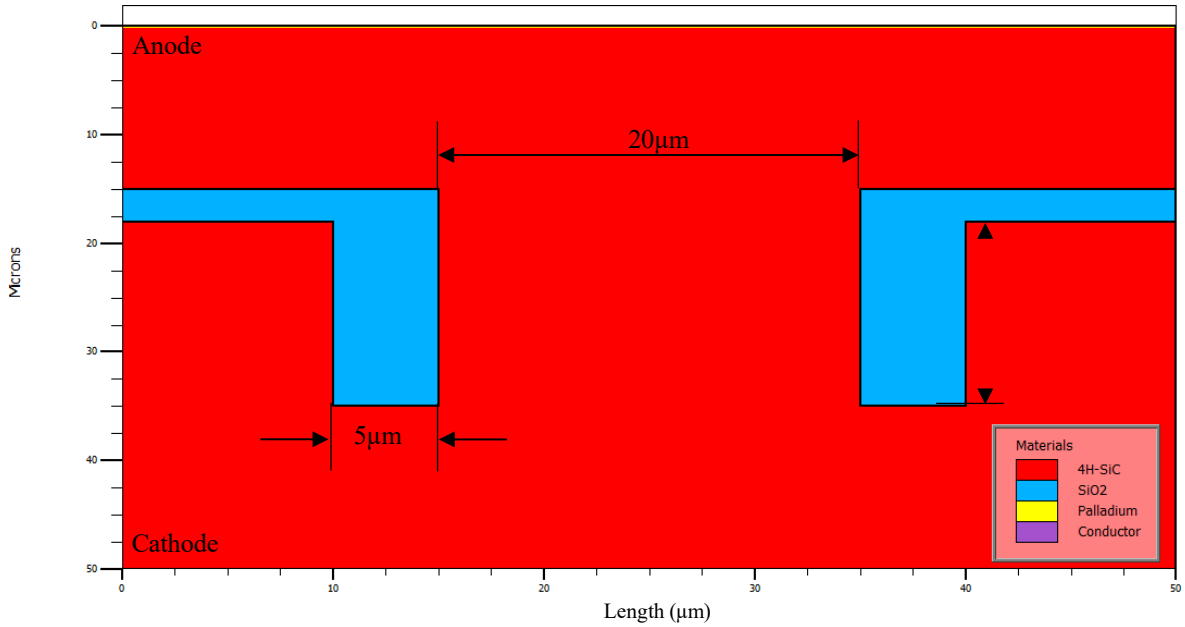

Figure 1. The structure of 4H-SiC-based Self-switching Diode (SSD).

The standard physical models of Shockley-Read-Hall (SRH) recombination, field-dependent mobility (FLDMOB), and AUGER recombination models were defined in the simulation [10] to consider the essential physical effects like recombination, mobility variation with the electric field, and carrier-carrier interactions. Furthermore, impact ionization (IMPACT SELB) was applied to account for the interaction between carriers and the crystal lattice under strong electric fields, resulting in carrier multiplication and potential breakdown events. Band to Band tunneling (BBT.STD) model was also added to account for the carriers directly tunneling across the energy barrier between valence and conduction bands. These models help to accurately predict device behavior near breakdown and optimize designs for enhanced reliability and performance in high-power devices [14–18].

Additionally, variations of the interface charge value from 10^{11} to 10^{13} cm^{-2}[19] in the dielectric SiO_2 layer and 4H-SiC epi-layer were performed to observe the effects of interface charge on the electrical characteristics of the device. The interface charge value is a key parameter that significantly impacts the current performance of devices, as it determines the forward current and reverse breakdown voltage of the target. Therefore, it is important to ensure that the interface charge density is consistent and well-controlled. Furthermore, variations in the type of the metal contacts using Molybdenum (4.2 eV), Palladium (5.5 eV), and Platinum (6.0 eV) materials were also performed to observe the relation of the metal work functions to the electrical performance in SiC-based SSD [10]. Finally, considering the broad spectrum of doping concentrations in 4H-SiC, which can span from 1×10^{14} cm^{-3} to 1×10^{19} cm^{-3} [20], this study also explores the range for an optimal value that yields enhanced electrical performance. In each instance of variation, all remaining unobserved parameters are held constant; the doping concentration at 1×10^{17} cm^{-3}, Palladium (5.5 eV) is utilized for metal contacts, and the interface charge is maintained at a level of 10^{13} cm^{-2}.

3. RESULTS AND DISCUSSION

The IV characteristics of 4H-SiC-based SSD were studied with different interface charge values, Schottky contact metals, and epilayer doping concentrations and are shown and discussed in the following subsections.

3.1 Variation in the Interface Charge Values

Variation of the interface charge density from 10^{11} to 10^{13} cm^{-2}, and the effects on the forward and reverse I-V characteristics are shown in Figures 2 and 3, respectively.

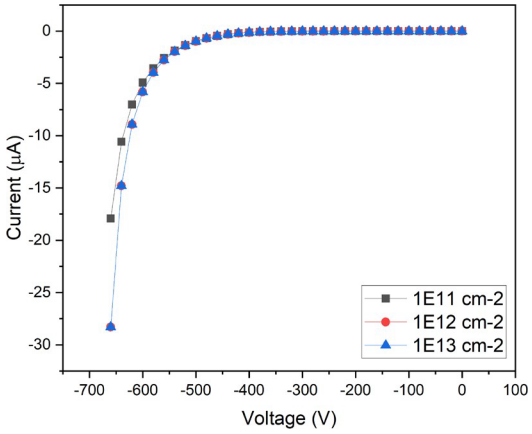

Figure 2. The IV characteristics of SiC-based SSD in reverse bias region with various interface charge values of 10^{11}, 10^{12}, and 10^{13} cm^{-2}.

The assessment of reverse leakage current and breakdown voltage are critical parameters that hold paramount significance due to their direct impact on the device's performance. As shown in Figure 2, it can be seen that the leakage current across all simulated interface charge values exhibited an incremental rise around the 550 V mark, further escalating beyond the 600 V threshold in reverse bias voltage. This signifies the cumulative impact of the interface charge-induced electric fields which contribute to carrier generation and influence carrier mobility, thereby leading to the observed rise in current. Specifically, for an interface charge of 10^{13} cm^{-2} the leakage current is highest at ~28 μA. However, importantly, this heightened leakage current did not significantly affect the breakdown voltage's initiation point highlighting that the interaction of electric fields caused by interface charge variation plays a minimal role in the device's breakdown mechanism.

On the other hand, the influence of varying interface charges on the forward current exhibit distinct behaviours. As shown in Figure 3, an evident trend emerges. With increasing interface charge values, there is a corresponding rise in the peak forward current generated by the device. This phenomenon can be attributed to the heightened concentration of charge carriers in the vicinity of the trench region. The observed behavior is intricately linked to the inherent Auger and Shockley-Read-Hall (SRH) recombination models, both of which exert a substantial influence on the recombination dynamics of charge carriers. Consequently, this interplay culminates in an expedited rate of carrier recombination kinetics [21]. This, in turn, results in more efficient energy release, ultimately contributing to a higher magnitude of current flow Notably, the most substantial interface charge value of 10^{13} cm^{-2} corresponds to the highest forward current observed, peaking at 2.75 A which strikes a favourable compromise between forward and leakage current values. It enables the device to effectively block voltages up to 600 V while concurrently sustaining a forward current of 2.75 A.

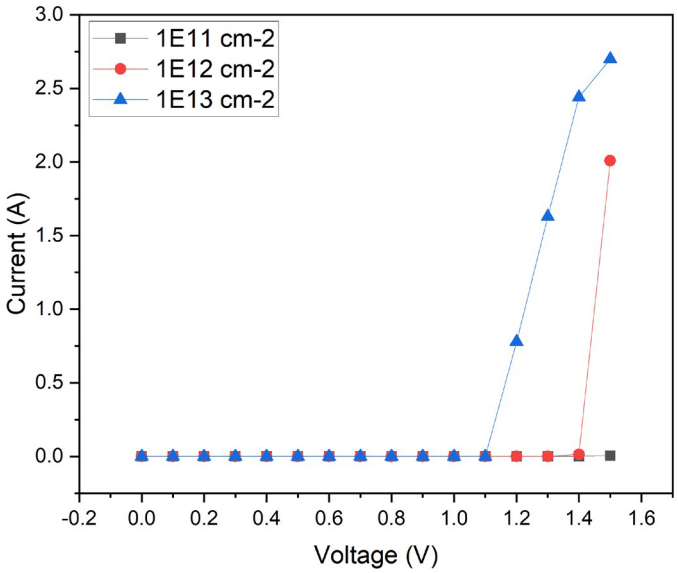

Figure 3. Forward current values of SiC-based SSD with various interface charge values of 10^{11}, 10^{12}, and 10^{13} cm^{-2}.

3.2 Variation in the Metals Contact and Work Function Values

Figure 4 illustrates the effect of different work function values for the metal contact in the SiC SSD, showing consistent breakdown voltage behavior at approximately 550 V in reverse bias before the device experiences breakdown. Additionally, the recorded highest reverse current of 30 µA at a reverse bias voltage of 650 V indicates that the device exhibits a degree of uniformity in breakdown behavior across different work function values. This suggests that the breakdown mechanism primarily involves the intrinsic properties of the SiC material and the device's structural design, rather than being critically influenced by the metal contact's work function.

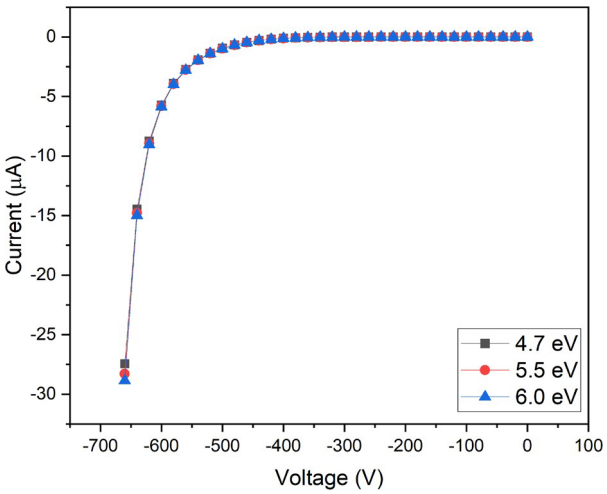

Figure 4. Breakdown voltage of SiC-based SSD with different Schottky metal contacts with work functions of 4.7, 5.5, and 6.0 eV.

Figure 5 illustrates the forward bias IV characteristics across different metal contacts. Notably, each work function value displayed unique patterns as bias increased up to 1.5 V. Strikingly, the molybdenum contact (with a work function of 4.7 eV) exhibited an intriguing behavior where its simulation failed to converge after 0.7 V, even with increased bias steps of 0.01 V. This inability to reach convergence raises questions regarding the underlying factors affecting the simulation's stability and the device's behavior. The convergence issue could potentially stem from the

complex interplay of material properties, carrier transport mechanisms, and simulation algorithms. Molybdenum's comparatively lower work function might influence the charge injection process into the semiconductor. As bias increases, electron injection becomes more demanding, particularly when the energy barrier at the metal-semiconductor interface poses a challenge. This can lead to the disruption of the numerical convergence process, potentially causing the simulation to stall or diverge [18].

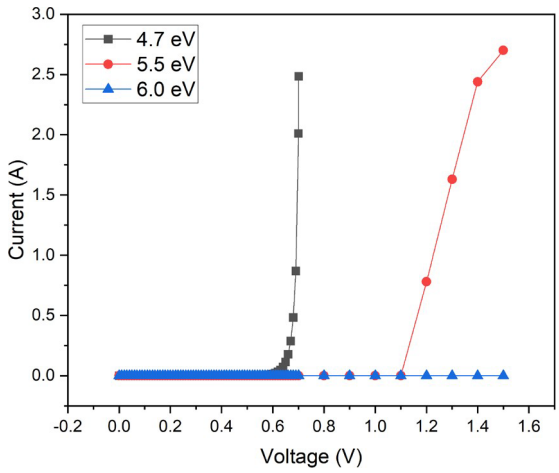

Figure 5. Forward current values of SiC-based SSD in various metal contacts with work functions of 4.7, 5.5, and 6.0 eV.

Meanwhile, a palladium contact (5.5 eV) yields the highest forward current of 2.5 A. A platinum contact (6.0 eV) results in a very minor forward current (around 7 nA) at the same bias of 1.5 V. In term of trend, it can be seen that the higher work function, as seen with platinum, leads to a lower voltage drop which might be caused by the higher energy requirement for extracting an electron, resulting in reduced current and voltage drop. This behavior suggests that the SSD is better suited for applications where current-carrying capacity is prioritized over high voltage tolerance. The diode's power rating of 1500 watts is derived from its 600 V blocking capability and 2.5 A current draw with the palladium contact.

3.3 Variation in Doping Concentration on 4H-SiC-based SSD

Figure 6 and Figure 7 show the IV characteristics with the variation in doping concentration in reverse and forward bias regions, respectively. In Figure 6, it is shown that the highest doping concentration of 10^{19} cm^{-3} started to experience leakage at ~550 V reverse bias with a further increased value of ~28 µA at 650 V reverse bias. On the other hand, the lower doping concentration values exhibited functional attributes even at 700 V reverse bias, successfully avoiding a breakdown. The observed trend can be understood by considering the role of doping concentration in shaping the electric field distribution within the device. A higher doping concentration leads to a more significant concentration of charge carriers, effectively increasing the availability of mobile charges within the semiconductor. Consequently, this elevated carrier density influences the way electric fields are distributed, enabling the device to withstand higher voltages before encountering a breakdown.

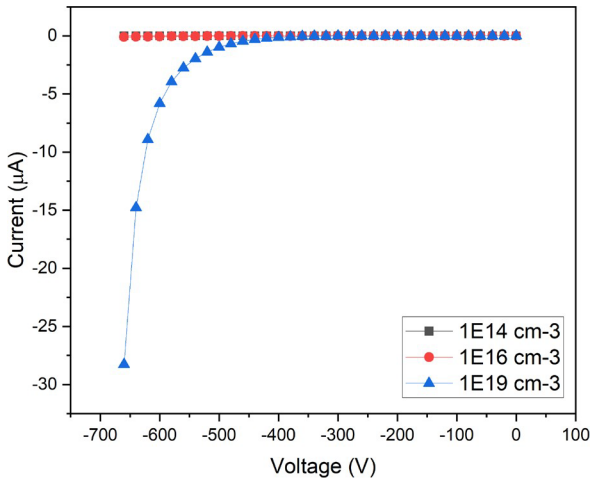

Figure 6. Breakdown Voltages at Different Doping Concentration Values for 10^{14}, 10^{16}, and 10^{19} cm^{-3}.

In forward bias region, the forward current performances improved significantly as the doping concentration increased, which is represented in Figure 7. At the lowest doping concentration, the forward current was negligible at the threshold voltage (0 V). However, with increasing doping concentrations, the forward current gradually increased, reaching 48 A at a bias voltage of 1.5 V. This behavior highlights a crucial relationship between doping concentration and forward current. As doping concentration increases, there is a rise in the concentration of charge carriers available for conduction, simultaneously facilitating improved forward current flow through the device.

Notably, this study shows that the SiC-based SSD exhibited a trade-off between breakdown voltage and forward current performance. Higher doping concentrations resulted in a narrower depletion region, leading to a higher breakdown voltage. Additionally, the device exhibits a significant increase in forward current with increasing doping concentrations. The synergy of a high breakdown voltage and a noteworthy forward current-carrying capacity gives rise to an impressive power rating of 27 kW for the diode. This exceptional power rating is derived from the diode's robust breakdown voltage, which is set at 600V, coupled with a forward current of 45A.

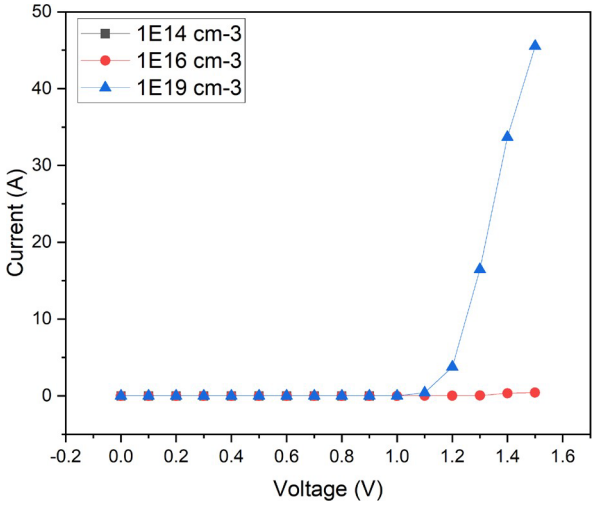

Figure 7. Forward currents values with different doping concentration values of 10^{14}, 10^{16}, and 10^{19} cm^{-3}.

4. CONCLUSION

An investigation into the electrical characteristics of SiC-based SSDs has been conducted, involving variations in interface charge, metal contact, and work function, as well as doping concentration values. The results demonstrated a trade-off between the electrical performance in the reverse and forward bias regions. The most notable alterations in electrical performance were observed through changes in the doping concentration of SiC, which shows the critical necessity for employing higher doping concentrations in future device fabrication. Significantly, the SSD displayed an impressive ability to endure a reverse voltage of 600 V and accommodate a substantial forward current of up to 45 A under a 1.5 V bias, leading to a remarkable high-power rating of 27 kW. These findings underscore the importance of optimizing the doping concentration in SiC-based devices together with interface charge and metal contact work function values to achieve desired breakdown characteristics and current-carrying capabilities. However, further analysis and validation should be considered with experimental works to achieve more accurate data. Further exploration in this domain holds considerable potential for advancing the development of high-voltage semiconductor devices for diverse industrial applications.

REFERENCES

[1] T. Yi Liang et al., Sensors, vol. 22, no. 24 (2022) pp. 9712.
[2] S. R. Kasjoo, Z. Zailan, N. F. Zakaria, M. M. Isa, M. K. M. Arshad, & S. Taking, "An overview of self-switching diode rectifiers using green materials," in AIP Conf. Proc., AIP, Sep. 2017.
[3] Z. Zailan, N. F. Zakaria, M. M. Isa, S. Taking, M. K. M. Arshad, & S. R. Kasjoo, "Characterization of self-switching diodes as microwave rectifiers using ATLAS simulator," in 2016 5th Int. Symp. on Next-Generation Electr., ISNE 2016, IEEE., Aug. 2016.
[4] N. F. Zakaria, S. R. Kasjoo, M. M. Isa, Z. Zailan, M. K. M. Arshad, & S. Taking, Bulletin of Electrical Engineering and Informatics, vol. 8, no. 2 (2019), pp. 396–404.
[5] Z. Zailan, N. F. Zakaria, M. M. Isa, S. Taking, M. K. M. Arshad, & S. R. Kasjoo, "Characterization of self-switching diodes as microwave rectifiers using ATLAS simulator," in 2016 5th International Symposium on Next-Generation Electronics, ISNE 2016, IEEE., Aug. 2016.
[6] M. B. M. Mokhar, S. R. Kasjoo, N. J. Juhari, & N. F. Zakaria, "An overview of semiconductor rectifier operating in the millimeter wave and terahertz region," in AIP Conf. Proc., 2020.
[7] S. Zhao, A. Kempitiya, W. T. Chou, V. Palija, & C. Bonfiglio, IEEE Trans. on Industry App., (2022), pp. 2965-2977.
[8] N. S. Hashim, B. Poobalan, N. F. Zakaria, M. Natarajan, & S. Shaari, Int. J. of Nanoelectronics and Materials, vol. 16, no. 1 (2023), pp. 177-185.
[9] S. K. Gupta, C. Shekhar, J. Akhtar, & N. Pradhan, IEEE Trans. on Semiconductor Manufacturing, vol. 25, no. 4 (2012) pp. 664-672 .
[10] R. Choudhary, M. Mehta, R. Singh Shekhawat, S. Singh, & D. Singh, "Optimization of a 4H-SiC Schottky diode using TCAD software," in Materials Today: Proceedings, 2021.
[11] J. Lee, K. H. Lim, & Y. S. Kim, Sci Rep, vol. 8, no. 1 (2018), pp. 13905.
[12] T. Yi Liang et al., Mathematics, vol. 10, no. 3 (2022), pp. 326.
[13] M. S. Kang, J. H. Lee, H. S. Lee, & S. M. Koo, J. Nanosci. Nanotechnol., vol. 13, no. 10, (2013) pp. 7042-7045(4).
[14] V. B. Sreenivasulu & V. Narendar, IEEE Trans Electron Devices, vol. 69, no. 8 (2022), pp. 4115 – 4122.
[15] M. Labed et al., ECS J. of Solid State Sci. and Tech., vol. 9, no. 12 (2020), pp. 125001.
[16] A. Gavoshani & A. A. Orouji, J. Comput Electron, vol. 20, no. 4 (2021), pp. 1513–1519.
[17] M. K. Anvarifard, IEEE Trans. on Device and Materials Reliability, vol. 16, no. 4 (2016), pp. 1530.

[18] S. Tripathi, Study of Sic-Based Neutron Detector for Applications in The Harsh Environment of Fast Reactors, in PhD thesis, Homi Bhabha National Institute, India (2019).
[19] Bejoy N. Pushpakaran, Modeling and Electrothermal Simulation of SiC Power Device, 1st ed. World Scientific (2019).
[20] Ionela-Roxana ARVINTE, Investigation of Silicon Carbide Based High Voltage And High Power Electronics Components, 2016.
[21] Y. Lv et al., ACS Appl Electron Mater, vol. 4, no. 11 (2022), pp 5487 – 5497.